Published in "Journal of Geophysical Research: Earth Surface
doi: 10.1002/jgrf.20069, 2013"
which should be cited to refer to this work.

Modeled sensitivity of two alpine permafrost sites to RCM-based climate scenarios

Martin Scherler,[1] Christian Hauck,[1] Martin Hoelzle,[1] and Nadine Salzmann[1]

[1] Climate change as projected by contemporary general circulation models (GCMs) and regional climate models (RCMs) will have a great impact on high latitude and high mountain permafrost. A process-based one-dimensional permafrost model is used to evaluate the sensitivity of two characteristic alpine permafrost sites to changes in climate for a 110 year time period starting 1991 and ending 2100 using output time series of six different GCM-RCM model chains. Statistical analysis of the RCM climate variables and output of the impact model has been conducted to gain insight into the sensitivity of the active layer to changes in climatic conditions. Strong sensitivity to climate change was found for the active layer thickness (ALT) at Schilthorn, which increased by up to 100% before most of the models pointed to a degradation of the permafrost around the year 2020. The sensitivity of the ALT at the rock glacier site Murtèl is less pronounced; permafrost degradation is slower and sets in only around 2070. At both sites, the thermal evolution is linked to an increase in unfrozen water content within the permafrost body. Multiple linear regression analysis shows a strong model dependency of ALT on ice content and summer soil surface temperatures and to a less significant degree on snow cover timing and duration. The ALT at Schilthorn is influenced by the ALT of the preceding year, while at Murtèl, the ALT is influenced by the ALT of up to 15 preceding years.

1. Introduction

[2] Permafrost as a thermal phenomenon of the subsurface is defined as lithospheric material having temperatures at or below 0°C for at least two consecutive years and is significantly influenced by the energy balance at the surface, the snow cover timing and duration, and precipitation.

[3] Observed changes in climatic variables and the projected continuing trends as consistently simulated by climate models [*Solomon et al*., 2007] have and will have important impacts on permafrost conditions. Observations from the past decades show increasing active layer thicknesses and ground temperatures in the Arctic and Scandinavia [e.g., *Romanovsky et al*., 2008; *Isaksen et al*., 2011], as well as increasing active layer thicknesses in the European Alps as a response to summer heat waves [e.g., *Hilbich et al*., 2008]. Talik formation [*Wu and Zhang*, 2008] and beginning permafrost degradation in Alpine scree slopes [*Phillips et al*., 2009] have also been reported. The latter two can lead to processes like thermokarst formation [*Kääb and Haeberli*, 2001; *Yoshikawa and Hinzman*, 2003; *Smith et al*., 2005] or the destabilization of steep debris slopes and rock walls, which, in turn, may provoke rock falls and debris flows [*Huggel*, 2008; *Huggel et al*., 2010], or cause instabilities to infrastructure [*Harris et al*., 2001a, *Arenson et al*., 2009].

[4] The effects of climate change on permafrost may be investigated for practical reasons related to natural hazards, or for pure scientific process understanding. Accordingly, a number of modeling approaches have been developed in recent years, each specifically constrained, e.g., by regional focus, data availability, computational power, or limited process knowledge. Spatially distributed models, which are used to assess the geographical extent of permafrost on large scales (e.g., circumarctic mountain ranges), often omit physical transient processes which are relevant on a more local scale [*Hoelzle et al*., 2001]. Such models include, for example, the statistical frost index method [*Nelson and Outcalt*, 1987], the analytical Stefan's solution for the heat transfer in solid media [*Lunardini*, 1981], the semi-empirical Kudryavtsev method [*Kudryavtsev et al*., 1974], N factors [*Lunardini*, 1978], the temperature at the top of permafrost model (TTOP) [*Smith and Riseborough*, 1996], and the statistical-empirical models PERMAKART [*Keller*, 1992] and PERMAMAP [*Hoelzle and Haeberli*, 1995]. Recent approaches aim at applying statistical models on Alpine-wide [*Boeckli et al*., 2012] or even global scales [*Gruber*, 2012]. An overview of many of these models can be found in *Riseborough et al*. [2008]. Also physically based

Additional supporting information may be found in the online version of this article.

[1]Department of Geosciences, University of Fribourg, Fribourg, Switzerland.

Corresponding author: M. Scherler, Department of Geosciences, University of Fribourg, Chemin du Musée 4, Fribourg 1700, Switzerland. (martin.scherler@unifr.ch.)

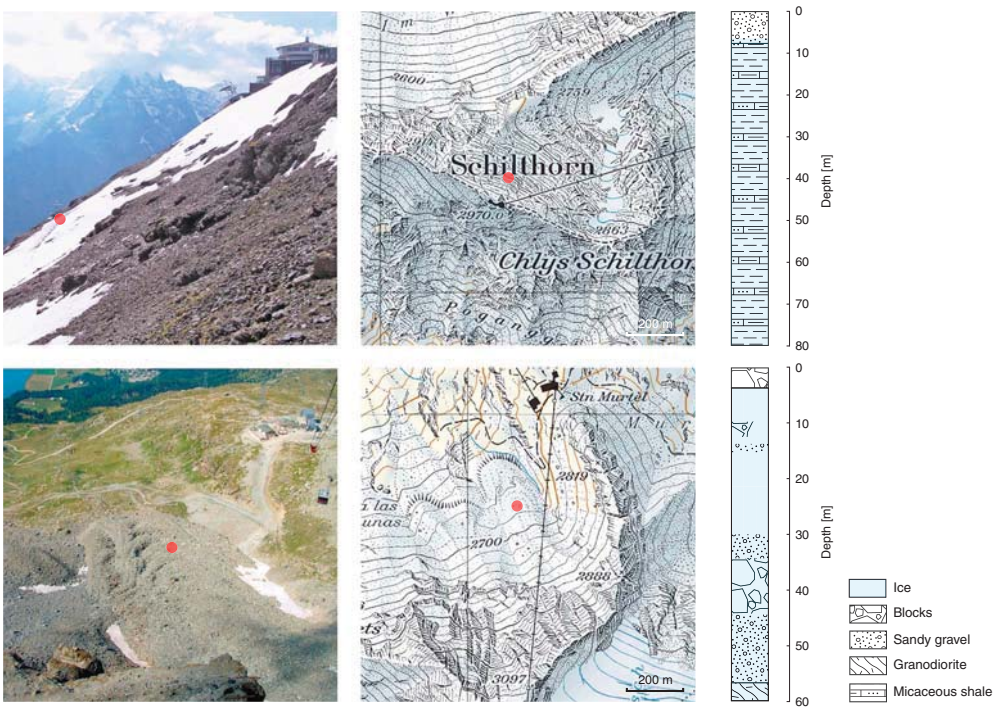

Figure 1. Field sites photographs, situation maps (reproduced by permission of swisstopo (BA13021)), and stratigraphy: (top) Schilthorn and (bottom) Murtèl.

2-D and 3-D models for frozen ground have been developed and applied so far [*Rigon et al.*, 2006; *Dall'Amico et al.*, 2011; *Lehning et al.*, 2006; *Voelksch and Lehning*, 2005]. Transient numerical models, which calculate soil temperature regime, ice, and water content on a large spatial scale still have a coarse spatial resolution like the contemporary general circulation models (GCMs) and regional climate models (RCMs) themselves, are computationally intensive and integrate only shallow soil layers (<10 m). If the focus of a study is on the transient response of a permafrost model to climate change scenarios, sophisticated soil models coupled with climate model output present a good alternative to study the hydrothermal evolution [*Salzmann et al.*, 2007; *Engelhardt et al.*, 2010; *Etzelmüller et al.*, 2011; *Luetschg and Haeberli*, 2005].

[5] In alpine terrain, the heterogeneity of the surface and the subsurface material, the complex terrain and the steep slopes, the corresponding data scarcity over larger regions as well as the complex interplay of thermal and hydraulic processes in a frozen but often permeable subsurface makes it difficult to apply a spatially distributed sophisticated model. One-dimensional approaches with sophisticated soil models have successfully been applied by, e.g., *Luetschg et al.* [2008] and *Scherler et al.* [2010]. The coupled heat and mass transfer model (CoupModel) [*Jansson and Karlberg*, 2004; *Jansson*, 2012; *Li et al.*, 2010] has shown to be well suited for simulating permafrost conditions in Alpine terrain [*Scherler et al.*, 2010; *Engelhardt et al.*, 2010].

[6] The objective of the present study is to simulate the hydrothermal regime at two characteristic alpine permafrost sites using the CoupModel driven by RCM scenario time series to (1) qualitatively evaluate the sensitivity of the hydrothermal regime to climate change scenarios, (2) use the gained data for a statistical sensitivity analysis of the active layer thickness (ALT), and (3) evaluate the sensitivity of both sites to climate changes, e.g., by analyzing the influence of ALT in preceding years on the ALT.

2. Study Sites

[7] This study concentrates on two extensively explored and well-instrumented high mountain permafrost sites in Switzerland (Figure 1): the Schilthorn summit in the Bernese Alps [*Imhof et al.*, 2000; *Hilbich et al.*, 2008; *Scherler et al.*, 2010] and the Murtèl-Corvatsch rock glacier in the Upper Engadine [*Haeberli et al.*, 1988; *Hoelzle et al.*, 2002; *Hilbich et al.*, 2009]. Both sites are part of the Swiss monitoring program PERMOS [*PERMOS*, 2010] and had been included in the European PACE project (1998–2001) [*Harris et al.*, 2001b]. They differ significantly from each other in terms of their climatic regime, topography, morphology, and surface and subsurface characteristics.

2.1. Schilthorn

[8] The Schilthorn massif is situated in the north central part of the Alpine arc. The site is characterized by a relatively thick layer (approximately 5 m) of fine-grained debris (see Table 1) over strongly jointed bedrock [*Hauck*, 2001]. Mean annual air temperature (MAAT, averaged over 1999–2008) is −2.6°C. Mean annual precipitation in the area is around 2700 mm [*Schwarb et al.*, 2001; *Mittaz et al.*, 2002]. The simulated 1-D profile discussed below (section 5) corresponds to the location of a 14 m deep borehole located on a narrow platform at 2900 m above sea level (asl) in the north facing slope, which is inclined by 30°, where temperatures are measured at different depths since 1998. The ALT at the borehole varied between 5 m and 9 m the beginning of the measurements in 1998. A farther borehole at 5 m distance confirms a permafrost thickness of

Table 1. Soil Properties

	Depth (m)	Grain Size Distribution (mm)							Porosity (%)
		<0.002	0.002–0.006	0.006–0.02	0.02–0.06	0.06–0.2	0.2–0.6	0.6– 2	
Schilthorn	0–0.5	7	4	7	10.6	25	12	34.6	45
	0.5–1.5	3	1	2	4	10	10	70	45
	1.5–3	0	0	0	0	10	20	70	35
	3–5	0	0	0	0	0	0	100	23
	5–100	0	0	0	0	0	0	100	5
Murtèl	0–0.1	0	0	0	0	0	0	100	10
	0.1–3.5	0	0	0	0	0	0	100	10
	3.5–30	0	0	0	0	0	0	100	85
	30–80	0	0	0	0	0	0	100	5

more than 100 m, with temperatures close to the thawing point (−0.5°C) at the bottom of the profile. The heat flux at the bottom of the borehole is nearly zero during the observation period from 1999 to 2008 (~0.002 W/m^2 between 90 m and 100 m depth).

[9] Beside thermal diffusion and latent heat processes in the subsurface, vertical infiltration of water from the melting snow cover has been shown to play a major role in the timing of seasonal active layer thaw in early summer, both in modeling [*Scherler et al.*, 2010] and in observational studies [*Hilbich et al.*, 2011]. The snow cover at the Schilthorn reaches maximum depths of about 3 m and usually lasts from October through to June. Simplified model sensitivity studies of *Engelhardt et al.* [2010] showed that caused by this late snowmelt and the long decoupling of the atmosphere from the surface, impacts of atmospheric changes would be strongest in summer, when increasing air temperatures could lead to an increase in ALT.

2.2. Murtèl-Corvatsch

[10] The rock glacier Murtèl-Corvatsch is located in the south eastern part of the Swiss Alps at 2670 m asl and is oriented NW. The study site is characterized by a layer of coarse boulders of approximately 3 m in thickness over a massive ice core reaching down 10 m to 20 m [*Arenson and Springman*, 2005]. The permafrost extends to the bedrock at a depth of about 60 m and its temperature lies between approximately −1.8°C in the ice core and near 0°C in the bedrock. ALT is typically around 3.5 m. MAAT was −1.8°C in the period from 1988 to 2006, mean annual precipitation is 2000 mm, and the average snow height is 0.41 m [*Hoelzle and Gruber*, 2008; *PERMOS*, 2009]. The heat flux at the bottom of the profile is negative (0.13 W/m^2) between the two lowest thermistors in 57 m and 58 m depth and 0.006 W/m^2 in an isothermal layer between 52 m and 57 m depth.

[11] Like for most rock glacier sites, the thermal regime at Murtèl rock glacier is strongly influenced by the extremely coarse blocky layer on top, which effectively insulates the ice core from the high air temperatures in summer. In addition, horizontal air flow in the blocky layer permits cold air to enter the active layer, which acts as an additional cooling effect [*Hoelzle et al.*, 1999; *Delaloye and Lambiel*, 2005]. On the other hand, conductive heat transfer is enhanced through the strong temperature gradient between the active layer and the ice core [*Schneider et al.*, 2011]. Infiltration of meltwater can play an important role in the blocky active layer, but lateral drainage is considered to be fast over large parts of the rock glacier (depending on slope angle) and most of the water will leave the system quickly on top of the ice layer [*Arenson et al.*, 2010].

3. Data and Models

3.1. Site Specific Measurements

3.1.1. Meteorological Time Series

[12] The meteorological time series used for the calibration consist of hourly in situ measurements of the variables 2 m air temperature, incoming short-wave radiation, incoming long-wave radiation, relative humidity, and wind speed (for details concerning the meteorological measurements, see *Hoelzle and Gruber* [2008]). Hourly values of precipitation have been obtained from meteorological stations of MeteoSwiss in the proximity of the study sites. For Murtèl-Corvatsch, the summit station at Piz Corvatsch, for Schilthorn, the stations of Mürren and Interlaken were used, corrected by the elevation difference as described in *Stocker-Mittaz et al.* [2002] and *Scherler et al.* [2010].

Table 2. ENSEMBLES Institutes and Models Used

	Institute	GCM	RCM
DMI	Danish Meteorological Institute	ARPEGE	HIRHAM
ETH	Swiss Federal Institute of Technology	HadCM3Q0	CLM
HC	Hadley Centre for Climate Prediction and Research	HadCM3Q0	HadRM3Q0
METNO	Norwegian Meteorological Institute	BCM	HIRHAM
MPI	Max-Planck-Institute for Meteorology	ECHAM5-r3	REMO
SMHI	Swedish Meteorological and Hydrological Institute	HadCM3Q3	RCA

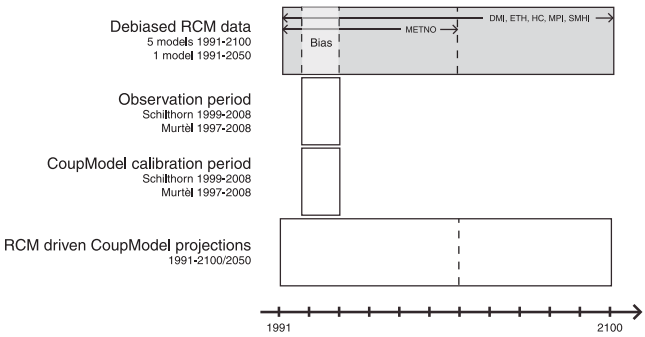

Figure 2. Diagram of the different models and the respective time periods used in this study.

3.1.2. Boreholes

[13] At both sites, borehole temperature data are available from thermistor chains which were lowered into the boreholes and equipped with sensors at different depth levels [*Haeberli et al.*, 1988; *PERMOS*, 2009]. At Schilthorn, there are three boreholes, one reaching 14 m depth and two reaching a depth of 100 m. One of the 100 m boreholes is drilled at an angle of 30° to the slope. At Murtèl rock glacier, three boreholes exist [*PERMOS*, 2009]. For this study, the data of the borehole with the longest record (drilled in 1987 and reaching a depth of 62 m) were used. Temperature data from this borehole are logged in 6 h intervals [*Hoelzle and Gruber*, 2008].

3.2. Climate Model Scenarios

[14] The climate change scenario data used to drive the subsurface model were obtained from the EU FP7 ENSEMBLES project [*Hewitt and Griggs*, 2004; *Van der Linden and Mitchell*, 2009]. This project yielded an ensemble of 20 transient regional climate models (RCMs) driven by five different global circulation models (GCMs) at their boundaries and forced by the A1B scenario from the Special Report on Emissions Scenarios [*Nakicenovic et al.*, 2000]. Most RCMs were run for the time window 1951–2100, with a few exceptions ending in 2050. The horizontal resolution of the RCMs generally was 25 km, with some exceptions of 50 km. A large number of output variables are freely accessibly through the data portal of the project (http://www.ensembles-eu.org/).

[15] For this study, we chose a set of six RCMs (each providing 25 km horizontal resolution) driven by three different GCMs (see Table 2). With the use of six different RCM-GCM chains, we consider to cover a reasonable part of the uncertainty range [e.g., *Fischer et al.*, 2011], while still keeping the number of time series used as input for the permafrost model at a manageable level. By including three GCMs, we furthermore accounted for the important role of boundary forcing in the final RCM output uncertainties [*Déqué et al.*, 2007]. The time span used for the impact modeling is 60 or 110 years starting in 1991 and ending in 2051 and 2101, respectively. Discrepancies of the time span simulated by the different models are due to differing calendars (that is, calendars with 365/366 days or 360 days) used by the models on the one hand and, in case of the short simulation period of 59 years, due to a limited simulation period of the RCM (until 2051). An overview over the models, validation periods, and RCM-covered time spans used in this study is shown in the schematic in Figure 2.

[16] The RCM output used in the present study was daily means (or sums) of the following variables: 2 m air temperature (tas), precipitation (pr), incoming short-wave radiation (rsds), incoming long-wave radiation (rlds), 2 m relative humidity (hurs), and 10 m wind speed (wss).

3.3. Soil Model

[17] The numerical model applied in this study for the simulation of the hydrothermal evolution of the active layer and the permafrost body is the one dimensional soil-snow-atmosphere-system model CoupModel [*Jansson and Karlberg*, 2004; *Jansson*, 2012]. The calculation of the coupled heat and mass transfer is based on fundamental physical equations and is extended by well-established empirical relations for the determination of the numerous thermal and hydrological soil and snow parameters. The model was already successfully applied for polar [*Hollesen et al.*, 2011] and mountain [*Engelhardt et al.*, 2010; *Scherler et al.*, 2010] permafrost sites.

[18] The upper thermal boundary condition is the result of a complete energy balance calculation. At the bottom of the profile, the energy flux is set to zero and water may leave the system by seepage flow. The zero heat flux at the bottom is regarded as a reasonable representation of the current conditions at the two sites (see section 2). Furthermore, we assume that (and also shown in Figure S2 in the auxiliary material where we applied a geothermal heat flux of 0.03 W/m^2) the geothermal heat flux virtually has no influence on the degradation at the top of the permafrost. The model integrates freezing and thawing processes (i.e., phase change of water) in the soil. At temperatures above a threshold temperature (−6°C), unfrozen water coexists with ice. This approach respects the fact that in porous media, liquid water coexists with frozen water at temperatures far below freezing point, due to high pressure build up inside small pore spaces during freezing [see, e.g., *Anderson et al.*, 1973]. Freezing processes in the soil are based on a function of freezing point depression and on an analogy of freezing-thawing and wetting-drying [see *Harlan*, 1973; *Jansson and Karlberg*, 2004]. Snow cover is simulated as one layer of variable height, density, and water content. Snow metamorphosis is simulated depending on the energy balance at the snow surface and various snow metamorphosis parameters (see detailed description of snow processes in the auxiliary material). Water transfer in the soil depends on texture, porosity, water, and ice content. Bypass flow through macropores is also considered. Lateral runoff occurs in saturated soil layers and at the surface, if infiltration capacity

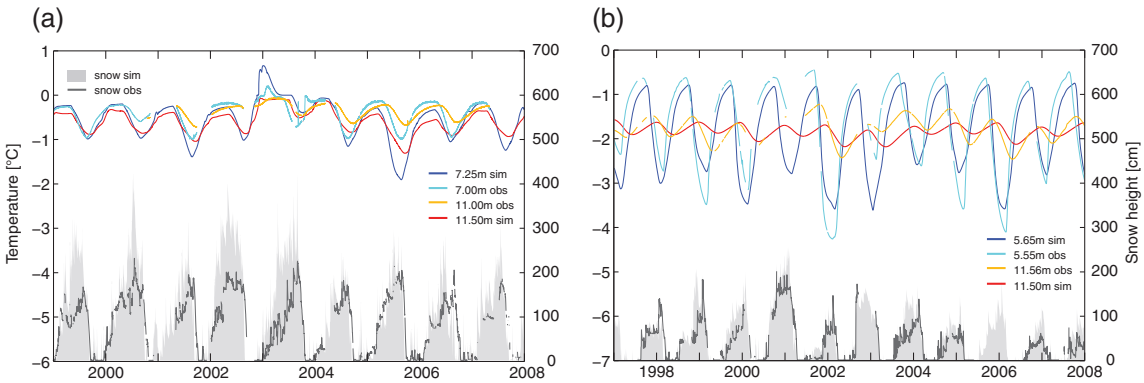

Figure 3. Simulated and observed temperatures at two depths and snow depth for the calibration period at (a) Schilthorn and (b) Murtèl.

is exceeded. Additional drainage is calculated by the Ernst equation to account for rapid lateral drainage in steep terrain [*Ernst*, 1956]. In the model, we assume that downslope lateral runoff will occur on the permafrost table. It is assumed that most of this runoff occurs at the same time as the vertical percolation (e.g., during snowmelt or precipitation events) at very fast rates and at a temperature near the freezing point, as the water has been in contact with the frozen ground slope upward.

[19] Soil characteristics have been estimated based on field observations. For the Schilthorn site, the estimation was additionally based on soil texture analysis of the surface material [*Scherler et al.*, 2010]. For the rock glacier Murtèl-Corvatsch site, a temporally active heat source/sink has been introduced in the upper part of the active layer to account for 3-D warming and cooling effects induced by rapid advection of meltwater and precipitation in spring and summer and ventilation in winter [*Hanson and Hoelzle*, 2003; *Hanson and Hoelzle*, 2004]. The maximum depth of the profile is 66.5 m for the rock glacier site Murtèl-Corvatsch and 82 m for the Schilthorn site. The profiles are divided into 50 layers. Layer thickness is increasing nearly exponential with depth, starting at the top of the profile with a thickness of 0.05 m and reaching 10 m at the bottom.

[20] Measured borehole temperatures and observations from an automatic weather station (AWS) of air temperature, incoming short-wave radiation, incoming long-wave radiation, relative humidity, wind speed, and snow height are used to calibrate and validate the model (cf. section 3.1.1).

4. Data Pre-processing and Post-processing

4.1. RCM De-biasing

[21] As the complex topography of mountainous terrain is not adequately reflected in the still relatively coarse horizontal resolution of the RCMs, it is necessary to adjust the RCM output to the study sites. This is done in two steps. In a first step, the climate model data of four grid cells closest to the study sites are considered. Then, the 2 m temperature time series of the four grid cells are subject to an altitude correction based on a simple lapse rate of 0.6°C/100 m. Based on the altitude-corrected temperatures, the best fitting grid cell for all parameters has been chosen as input for the impact simulations. In a second step, the data were de-biased. Two different de-biasing approaches have been developed and proven for local permafrost studies in the Alps, the so-called delta and bias approaches [*Salzmann et al.*, 2007]. Here we applied a modified form of the bias approach. For this, the differences between the seasonal (DJF, MAM, JJA, SON) averages of the model output and the observations for a 10 and 11 year period, respectively, determine the bias. The periods were chosen according to the longest available consistent observation period for each site (1999–2008 Schilthorn, 1997–2008 Murtèl). The time series from the climate models were then adjusted by applying the relative seasonal bias.

4.2. Sensitivity Analysis

[22] Permafrost is subject to various processes and influencing factors leading to an annual variability of the ALT. The ALT itself is a proxy of the energy balance and the prevailing hydrothermal regime. Based on output data of the 110 year simulation runs of the permafrost and the active layer at the two sites, a multiple regression analysis was applied to gain insight into the role of often discussed influencing factors (such as snow cover, ice content, or summer surface temperature) on ALT [e.g., *Luetschg et al.*, 2008; *Engelhardt et al.*, 2010]. Eight potential influencing factors have been chosen for the sensitivity study: soil surface temperature in summer/early fall (July, August, September; JAS), snow cover duration (snow cover >1 cm), snow cover duration (snow cover >50 cm), onset

Table 3. Correlation Coefficients for the Calibration Period

Murtèl	0.55 m	2.55 m	5.55 m	10.55 m	11.55 m	Snow
Pearson r	0.88	0.84	0.86	0.71	0.54	0.88
Schilthorn	0.2 m	1.2 m	5.0 m	7.0 m	11.0 m	Snow
Pearson r	0.79	0.90	0.86	0.84	0.73	0.82

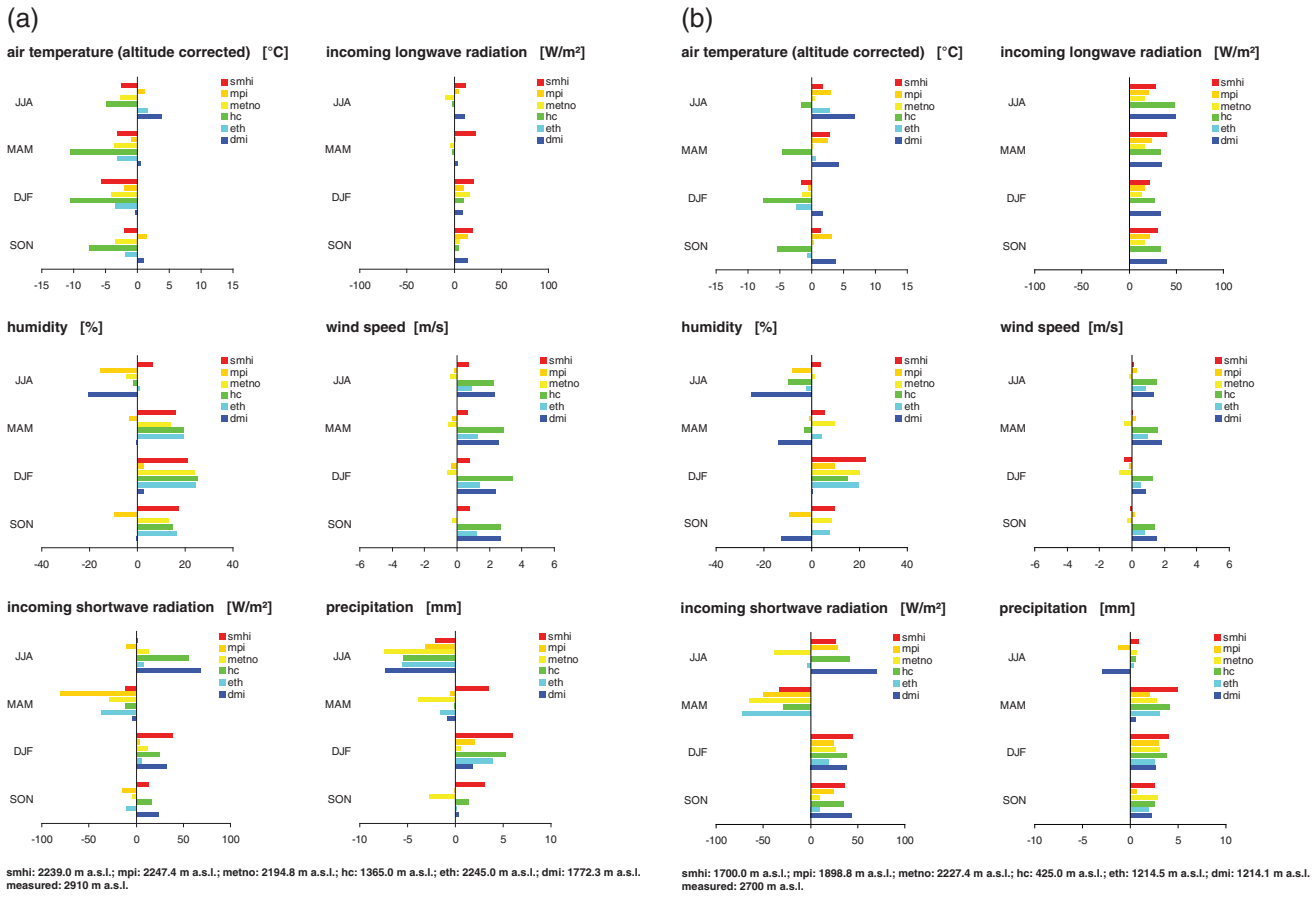

Figure 4. Biases of the RCM parameters with respect to the measurements at the study sites for the period of 1999–2008 ((a) Schilthorn) and 1997–2008 ((b) Murtèl).

of snow cover in fall (day of year; doy), onset of snow cover (snow cover >50 cm) (doy), day of becoming snow free (doy), air temperature (JAS), and ice content of the active layer prior to annual thawing. The snow cover threshold of 50 cm was chosen as an average value of the results of different studies giving ranges between 30 cm and 80 cm for insulation effects of the snow [e.g., *Hanson and Hoelzle*, 2004; *Schneider et al.*, 2011; *Luetschg et al.*, 2008]. Only years showing a complete refreezing of the active layer were considered.

[23] A multiple linear regression using ALT as the dependent variable and the eight influencing factors as independent variables was computed to evaluate the relative importance of these factors for ALT. The assessment of the importance of each variable for the regression was based on the stepAIC function of the MASS package [*Venables and Ripley*, 2002] of the software R [*R Development Core Team*, 2008]. R is an open source statistical software and programming language, similar to the commercial software S [*Venables and Ripley*, 2002], widely used in science for statistical analysis. The MASS package provides basic statistical functions and data sets for *Venables and Ripley* [2002]. The relative weight of the independent variables on the regression was then evaluated using a bootstrap process within the "relaimpo" package [*Grömping*, 2006] to calculate the metric Lindeman-Merenda-Gold (LMG) [*Lindeman et al.*, 1980] which is a measure for the relative importance of the regressors in the linear model. This metric decomposes R^2 into nonnegative contributions that automatically sum to the total R^2. The approach taken by the metric LMG [*Lindeman et al.*, 1980] is based on sequential R^2 values but takes care of the dependence on orderings by averaging over orderings using simple unweighted averages [*Grömping*, 2006].

[24] Results from monitoring studies analyzing measured ALT suggest a memory effect of the active layer in respect of thawing conditions of preceding years [*Hilbich et al.*, 2008]. Here we used the simulated ALT to perform a correlation of ALT in 1 year and ALT in the preceding 1 to 15 years.

5. Results

[25] The results comprise an analysis of the results for the model calibration period, an analysis of the time series of the relevant meteorological variables from the RCM simulations, the analysis of the permafrost impact simulations as well as the statistical sensitivity analysis.

5.1. Calibration of the Soil Model

[26] In case of the Schilthorn, the calibration of the soil model was based on borehole data and information gained during drilling of the three boreholes as well as laboratory analysis of the top soil. Water content and porosity were taken from the latter and extrapolated for the fine-grained layer [*Scherler et al.*, 2010]. For Murtèl rock glacier, subsurface parameters were estimated based on data from the drill

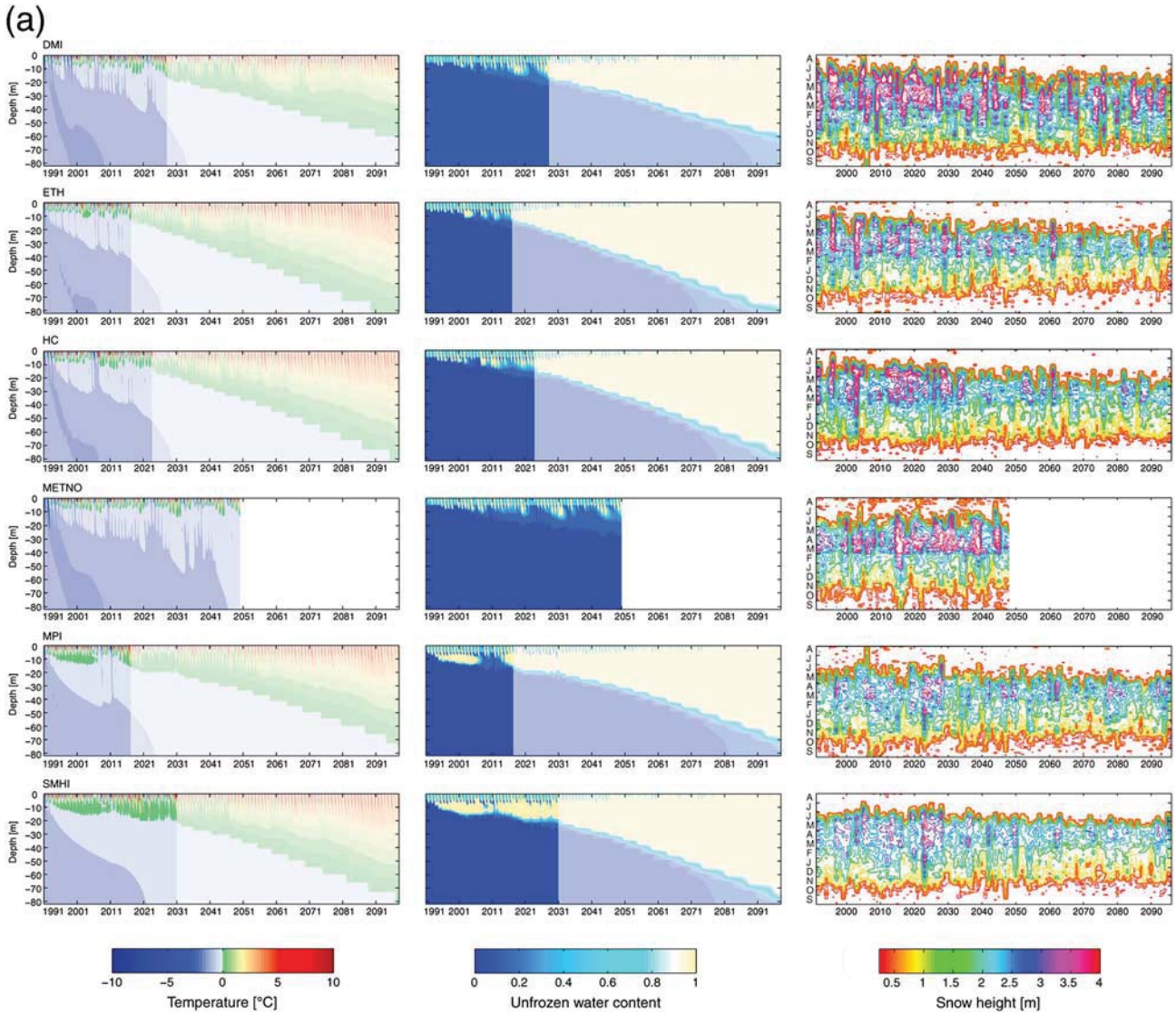

Figure 5. Simulations of the hydrothermal regime during the late 20th and the entire 21st century for (a) Schilthorn and (b) Murtèl illustrated by the (left) temperature evolution and the (middle) liquid to total water ratio. The plots have been faded after the point degradation sets in due to high uncertainties in the subsurface properties. (right) The corresponding snow cover timing and duration are shown with the snow depths as contour lines starting at a depth of 25 cm (bold line indicates a snow cover of 50 cm depth).

core analysis of three boreholes [*Vonder Mühll and Holub*, 1992; *Arenson et al.*, 2002]. Initial temperatures were chosen as constant over the entire profile (−0.7°C for Schilthorn and −1.5°C for Murtèl). Total water contents, as estimated for the two sites, are transferred into ice and liquid water content based on initial soil temperatures prior to the start of the model assuming thermodynamic equilibrium conditions.

[27] The soil model is calibrated with 10 year (11 year for Murtèl) simulations using observed meteorological parameters from the study site as input and borehole temperature measurements for validation. Figure 3 shows the results of the calibration process for temperature at two different depths together with the snow height. Discretization of the soil model and thermistor depth intervals (50 cm to 1 m) is not exactly harmonized, so the values of the model soil layers nearest to the respective thermistors are shown. On both sites, the snow cover is simulated reasonably well by the model (see Table 3). The maximum snow height is slightly overestimated, but especially the time of onset and complete meltoff of the snow cover matches the observations by a few days on average.

[28] Ground temperatures are shown for two depths for both sites. Temperatures below 5 m have been chosen for calibration in respect of the long-term atmospheric warming, which is considered to have the largest impact at these depths. Correlation coefficients for five depths are shown in Table 3. In most years, the subsurface temperatures at Schilthorn are slightly underestimated by the model. The largest deviations occur during the cold periods. An

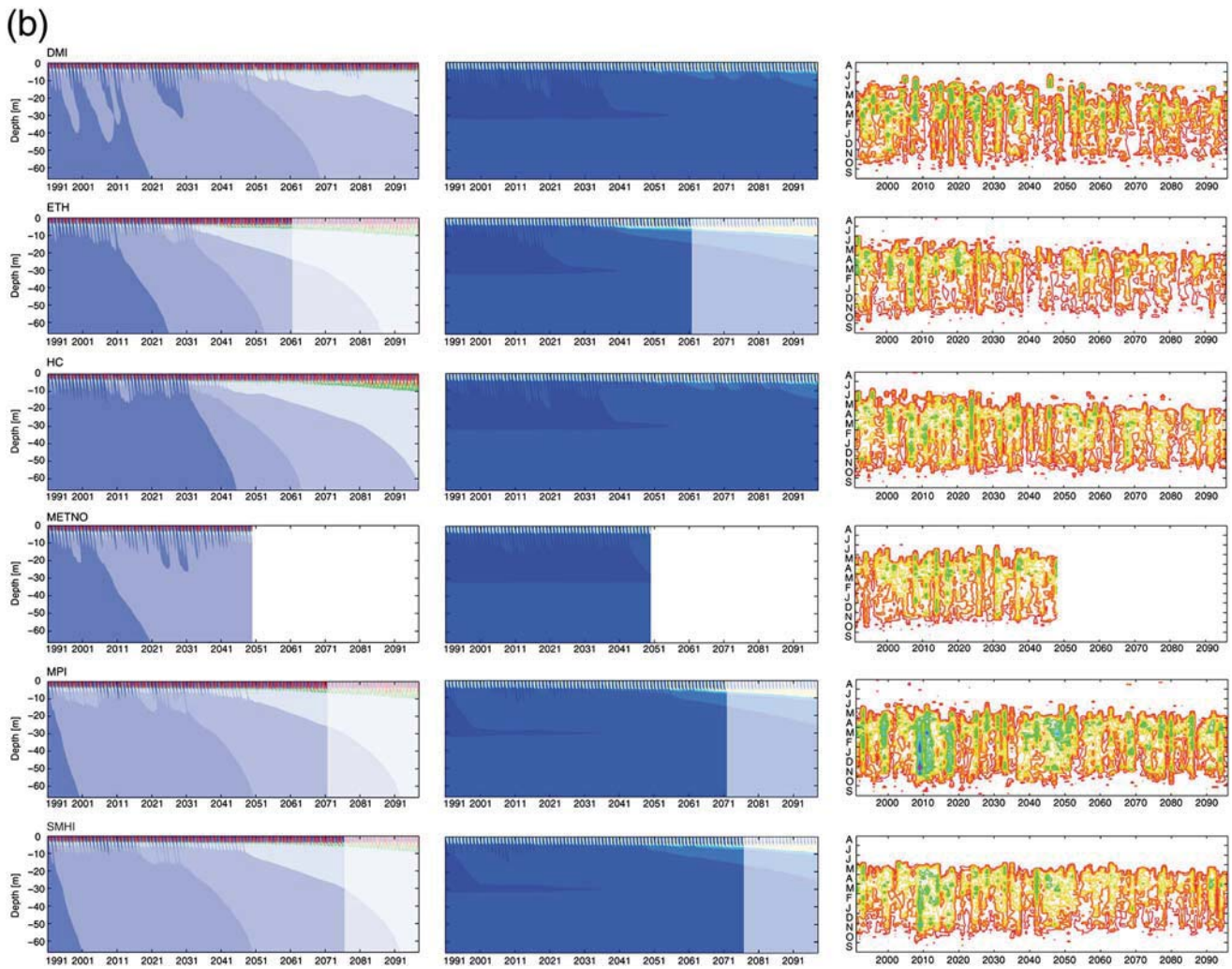

Figure 5. (continued).

overestimation is seen for the exceptionally warm summer of 2003. At Murtèl, the temperature amplitudes are smaller in the model compared to the measurements during most of the simulated period. The average temperatures below 10 m are simulated with reasonable accuracy (0.005–0.050 K) although correlation coefficients are declining with depth due to a phase shift in minimum and maximum amplitudes. The shift of the phase lag is a function of the ice content in the model, which can be very heterogeneous in alpine permafrost terrain. With respect to the long-term simulations, we chose comparatively high ice contents as conservative assumption (see Figure S1 in the auxiliary material with simulation results using different ice contents in the permafrost).

5.2. RCM Meteorological Output

[29] The 110 year daily mean ENSEMBLES RCMs output time series have been compared to the observations on a seasonal time scale to obtain the respective biases for each parameter. The results of this analysis are shown in Figure 4. In general, substantial seasonal biases are found for all of the six parameters. The RCMs perform differently for the two sites, but some similar patterns and consistent deviations can be found. The interseasonal variations found in most of the model parameter biases are not necessarily consistent between the models.

[30] For incoming long-wave radiation, almost all models show a positive bias of up to 50 W/m^2 for all seasons and both sites (somewhat more pronounced for Murtèl). For wind speed, similar consistent deviations are found. In general, too high values of wind speed are evident at both sites and for most models. For Schilthorn, MPI and METNO, however, show slightly too low wind speed almost all year round. This is also apparent for Murtèl during winter, where METNO, MPI, and SMHI show too low wind speed values.

[31] Overall, similar patterns of deviation are also found for incoming short-wave radiation, at both sites and for all models and with clear seasonal differences. While most models show clear positive biases for JJA, DJF, and SON, all models at both sites show negative biases of the same magnitude for MAM. Similarly, for relative humidity, most models show for both sites a positive bias for three seasons (MAM, DJF, and SON) but a mostly negative bias for JJA.

[32] For precipitation, there are also some obvious deviations found, although somewhat less consistent in terms of models, seasons, and sites. During JJA, all models show a clear deficit in precipitation at Schilthorn. Although at

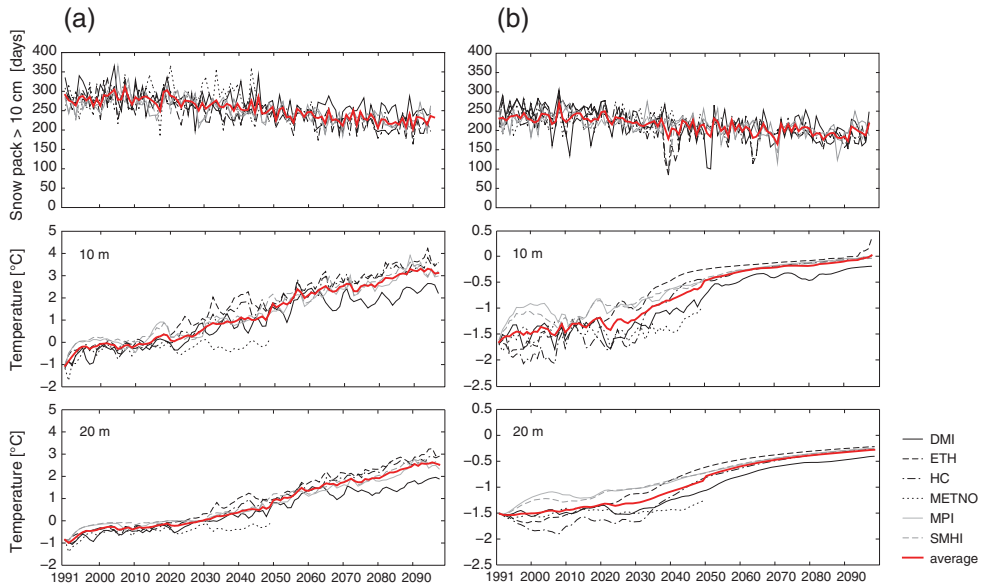

Figure 6. Simulated annual snow cover (>10 cm) duration and simulated ground temperatures at 10 m and 20 m depth from 1991–2100 at (a) Schilthorn and (b) Murtèl rock glacier as modeled with CoupModel driven with six different RCMs.

Murtèl, DMI and MPI also show a (smaller) deficit, the remaining models even show a slight positive bias. At both sites, most models show a clear positive bias of up to 5 mm for the remaining seasons. This is more consistent at Murtèl than at Schilthorn, where some models also show negative biases during MAM and SON.

[33] Biases found for air temperature are much more diverse compared to the other variables, particularly for Murtèl, where no consistency between models and seasons can be found. At Schilthorn, more consistent biases are found, with most models showing a clearly negative bias for air temperature almost all year round. Notable for air temperature (after altitude correction) are also the high negative biases of up to 10°C (!).

[34] Finally, some consistent patterns are seen in the RCM output variables analyzed in the context of this study independent of the RCM used and the site, i.e., biases in incoming short-wave radiation and precipitation. RCM short-wave radiation is underestimated in spring whereas it is overestimated during the other seasons. Precipitation is underestimated or constant in summer and higher during winter.

5.3. Climate Sensitivity of Permafrost

[35] We focus on the thermal regime, the ratio of liquid water to total water (including ice), and the snow cover timing, duration, and height for the simulated period from 1991 to 2100 (Figure 5) to analyze the sensitivity of the permafrost evolution at the two sites to climate scenarios as projected by the ENSEMBLES RCMs.

[36] The snow cover evolution is shown in the right column in Figure 5 depicting snow height contour lines as a function of year (x axis) and day-of-year (y axis). The months on the y axis are centered on the winter months with the largest snow cover. The outermost line indicates a snow cover of 25 cm, and the bold red line indicates a presumably insulating snow cover of 50 cm [e.g., *Zhang et al.*, 2001].

[37] The simulated snow cover shows a general decrease in duration of about 50 to 80 days during the 21st century (September–June at the beginning of the simulation and October–May at the end; cf. Figures 5 and 6). The onset of the snow cover is delayed, and the time when the sites become snow free is earlier than observed in recent years. At the Murtèl site, the model results show a number of years during the entire simulation period with no persisting snow cover of more than 25 cm height. The plots of subsurface temperature and unfrozen water content show two distinct phases of the evolution of the hydrothermal regime in warming permafrost. The first phase (Phase 1) is characterized by a slow warming trend of the permafrost body below a slightly increasing active layer, intermitted by periods of inactive permafrost conditions and the absence of complete refreezing in winter. The subsequent second phase (Phase 2) marks the beginning of permafrost degradation by gradually increasing thaw layer depth above the permafrost body, the latter remaining at temperatures near 0°C.

[38] At the Schilthorn site, the first phase starts at the beginning of the simulation in 1991 and lasts for two to six decades. During this period the scenarios of DMI, ETH, and HC project an active layer with depths varying from 5 m to 12 m. In the scenarios of MPI and SMHI, this period is intermitted by inactive permafrost conditions, as can be seen more clearly in the liquid to total water ratio plots, where a zone of unfrozen water above the permafrost table persists 11 to 14 years. After this period, a short interval of interchanging active and inactive permafrost conditions in certain years can be observed. Only in the METNO scenario, the first phase lasts until the end of the simulation period, with increasing liquid water in the top 30 m of the permafrost.

[39] At the Murtèl site, the first phase persists longer: between six decades in the case of the short scenario METNO and over the entire 21st century in the case of the DMI scenario. In the scenarios of ETH, HC, MPI, and SMHI,

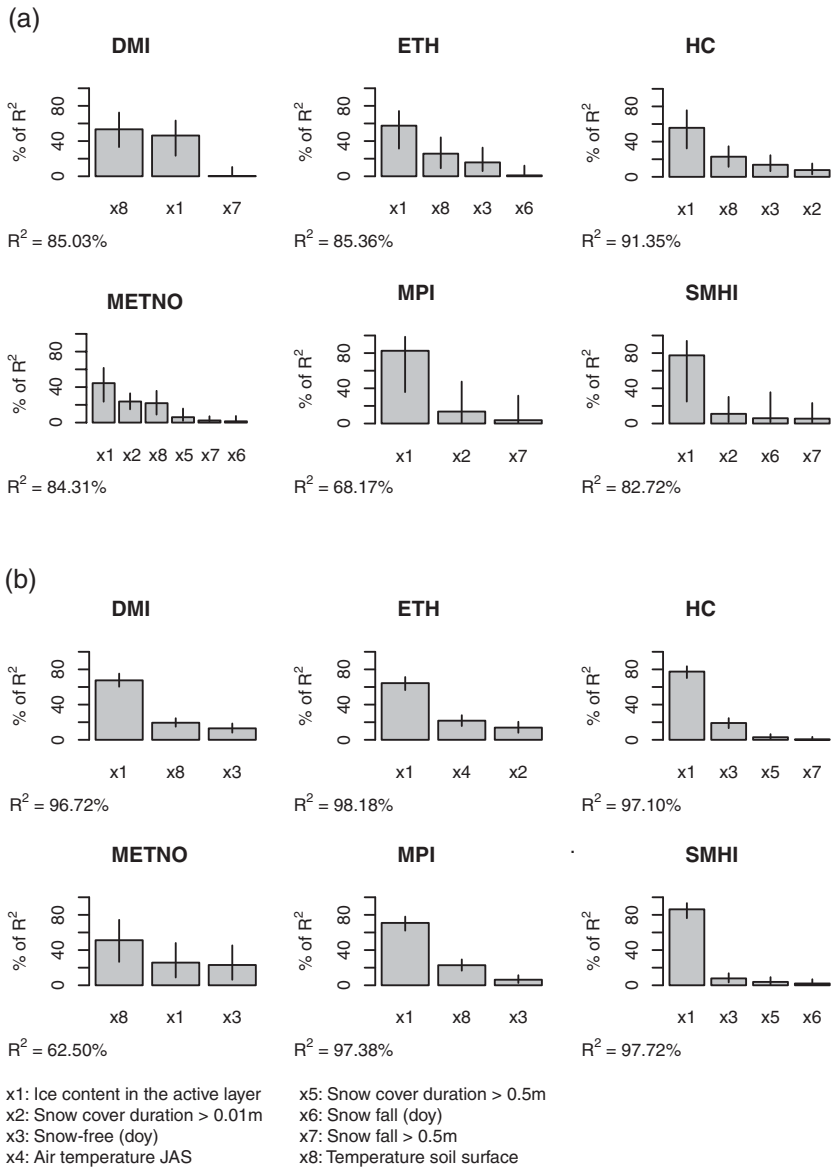

Figure 7. Bar plots of the metric LMG [*Lindeman et al.*, 1980] depicting the relative importance of selected variables for the multiple linear regression model explaining the simulated active layer thicknesses for (a) Schilthorn and (b) Murtèl. The metrics are normalized to sum 100%. The error bars indicate the 95% bootstrap confidence intervals.

this phase consistently lasts for eight decades. The active layer thickness increases from 3.5 m to 7 m during this period, and the liquid to total water ratio in the ice rich layer increases.

[40] Figure 6 (bottom) shows the temperature development in 10 m and 20 m depth at the two sites. When temperatures are close to 0°C, a zero curtain effect can be seen at both sites. This effect is more pronounced at the rock glacier site due to much higher ice contents in the respective model layers.

[41] Comparing both sites, it can be seen that the second phase starts five decades earlier at Schilthorn than at Murtèl for the ETH, HC, MPI, and SMHI scenarios. The DMI scenario at Murtèl and METNO scenario at both sites end before the onset of the second phase, i.e., no severe permafrost degradation is simulated.

5.4. Sensitivity Analysis

[42] From the eight potential influencing variables described in section 4.2, the stepAIC procedure (for stepwise selection of the regressors) selected three to seven (out of eight) dominant regressors in the case of Schilthorn and three to six dominant regressors in the case of Murtèl. The relative importance (in % of the respective R^2 value, normalized to sum 100%) of each regressor for the regression model, evaluated with bootstrapping, is shown in Figure 7. The most important regressors in the model, with regard to the independent variable ALT, are, according to this method, the ice content in the active layer prior to seasonal thawing, the JAS temperature of the soil surface followed by the snow cover duration >0.01 m, and the day of complete melt out of the snow cover. The regression models obtained through this procedure show R^2 values of 0.68 to 0.91 for Schilthorn and 0.60 to 0.98 for Murtèl,

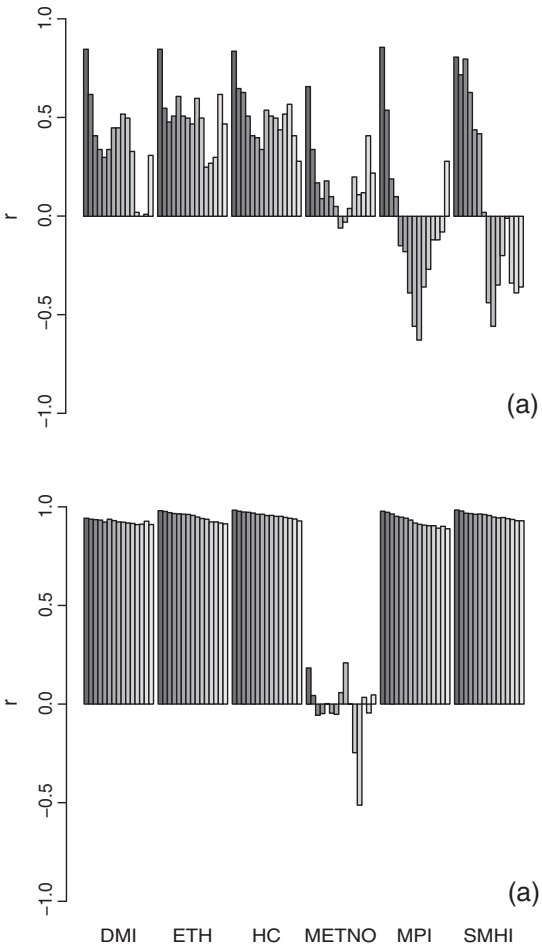

Figure 8. Correlation coefficients between the ALT in the year t and the ALT in the year $t - i$ for $i = 1$–15 years at (a) Schilthorn and (b) Murtèl.

representing a measure of the fit of the linear regression. The importance of the ice content on ALT has also been stressed by *Zenklusen and Phillips* [2012].

[43] At both sites, the ice content in the active layer was the most important regressor for all models except for DMI (Schilthorn) and METNO (Murtèl), where soil surface temperature was the most important factor in the statistical model.

[44] Figure 8 shows the correlation coefficients between ALT at time $t - i$ and ALT at time t, where $i = 1, \ldots, 15$, and t and i are given in years. High and positive correlation coefficients point to a strong relation between the active layer thicknesses in consecutive years. The maximum number of data points in each model decreases from n to $n - 15$ at $t = 15$ years. In the case of Schilthorn, data gaps exist in years with inactive permafrost conditions, as the active layer thickness is not defined then. The minimal number of data points (i.e., years which can be used for the correlation) is 14 for the SMHI scenario at Schilthorn, the maximum number is 105 for the DMI scenario at Murtèl. At Schilthorn, the correlation between ALT at $t - i$ and ALT at t is very strong for the first year for all models except METNO. Subsequent coefficients show no clear signs of decreasing correlation strength in time but a rather random signal. For the longer time spans in MPI and SMHI, even negative correlations occur. At Murtèl, the initial correlation coefficients are very high, and the signal in the subsequent years shows a slowly decreasing trend, except in the METNO model. This trend persists 15 years with decreasing correlation strength for increasing i.

6. Discussion

6.1. Calibration

[45] The snow representation during the calibration period is considered as reasonably fair. Above a snow height of around 60–100 cm, the absolute snow height is not important thermally [see also *Hoelzle et al.*, 1999; *Luetschg et al.*, 2008; *Scherler et al.*, 2010]. On the contrary, the beginning and end of the snow-covered period are very important, and they are well modeled in both cases.

[46] The high simulated temperatures during the hot summer 2003 at Schilthorn are, to a large degree, due to discretization effects. In Figure 3, we plotted a depth level very close to the active layer maximum. If this is overestimated/underestimated by a few centimeters, the temperatures directly above that level are much higher than the observations, due to an abrupt absence of latent heat effects. If depth levels well above or below the active layer maximum are analyzed the match is much better (see Table 3). We show the calibration close to this level to capture the maximum deviation of the model. For these reasons, we believe that long-term simulations can be performed with the model—however, the results should be regarded in the context of permafrost sensitivity and not as a prediction when degradation is starting to occur.

[47] Certain years during the calibration period for the Schilthorn site show an underestimation of ground temperatures. This underestimation is not consistent with the uncertainties of the maximum simulated snow cover heights (see, i.e., the winters 2004/2005 and 2005/2006) where the snow cover is simulated with good precision but the minimum soil temperatures are underestimated only in the winter 2005/2006. This rather points to problems in the soil parameterization, showing that more efforts have to be made regarding subsurface data collection (other than temperature) in high mountain terrain to obtain a realistic parameterization of the soil properties.

6.2. Impact Modeling

[48] When analyzing the impact of climate forcing on soil hydrothermal regime in a pure modeling approach, the uncertainties of the respective models have to be considered before being able to interpret the results in a meaningful way. In this study, we used climate variables from RCM output driven by GCMs to run a one-dimensional soil model. Possible errors can originate from various sources and can be propagated through the whole model chain. The uncertainties of both GCMs and RCMs are broadly discussed in literature [e.g., *Murphy et al.*, 2004; *Hawkins and Sutton*, 2009; *Christensen et al.*, 2007]. In this study, these uncertainties are at least partially accounted for by using climate data originating from six different GCM-RCM combinations which are expected to reflect a significant portion of the model uncertainty ranges. Nevertheless, uncertainties arising from limited process understanding, from the assumptions of the emission scenarios, from the

coarse spatial resolution, etc., in climate models may exist and will remain, if their output is used in impact studies.

[49] For the impact model, the main sources of uncertainties are the soil hydrological and thermal properties, which to a large extent cannot be obtained from field measurements but have to be estimated in the calibration process.

[50] The ground thermal regime and the snow cover conditions simulated during the calibration process, using measured data of meteorological variables and borehole temperatures over a period of 11 years at Murtèl and Schilthorn, fit the measured values soundly. Nevertheless, the results of this modeling study show the sensitivities of permafrost evolution to RCM-based climate change scenarios at two representative alpine permafrost sites. The results should not be interpreted as predictions of future permafrost evolution.

[51] ALTs of up to 12 m as seen in the simulations of the Schilthorn site could be explained by the small porosity and low water content in the rock material (see Table 1) which leads to smaller amounts of latent heat released during freezing.

[52] The advantage of the combination of a sophisticated soil model and climate model output is that important processes governing the hydrothermal regime in the permafrost (infiltration, percolation, freezing, and thawing, effects of unfrozen water) are simulated in more detail and to larger depths than within the integrated soil layers of climate models themselves. Disadvantageous on the other hand is the fact that effects such as latent heat phenomena and albedo changes are not directly coupled between the soil and the atmosphere and that with the model applied only 1-D modeling is possible. RCMs on the other hand, include a shallow soil column, which at least roughly accounts for coupling effects between the ground and the atmosphere.

[53] With respect to the rock glacier Murtèl, the initial thermal conditions beneath the ice core at depths below 30 m are warmer in reality (0°C to −1.5°C) than in the soil model (−1.5°C). This is due to the fact that the soil model is initialized assuming a constant soil temperature over the entire profile. Therefore, the thermodynamical equilibrium conditions are given by this assumption resulting in the fact that ice and unfrozen water coexist at a certain ratio according to the initial temperature [*Jansson and Karlberg*, 2004; *Scherler et al*., 2010]. Thus, these temperatures are underestimated at the start of the simulation and warming will be delayed compared to conditions in nature. In addition, the lower thermal boundary condition of the soil model consists of a zero heat flux. At both sites, a zero heat flux from the bottom is close to the real conditions at 85 m/60 m depth as measured within the boreholes [*PERMOS*, 2010].

[54] At Murtèl, an additional heat source in spring and summer (June to mid-September) had to be introduced into the model, accounting for rapid warming due to infiltration of meltwater as well as a heat sink for the period of mid-September to January to account for convective energy exchange through air in the blocky layer above the ice core of the rock glacier [*Hoelzle et al*., 1999; *Mittaz et al*., 2000; *Hanson and Hoelzle*, 2004]. For simplicity, this source/sink term was chosen to be constant over the respective periods, which is certainly a simplification as measurements within the blocky layer have shown considerable temporal variability of these advective and convective fluxes (M. Panz, Analyse von Austauschprozessen in der Auftauschicht des Blockgletschers Murtèl-Corvatsch, Oberengadin, unpublished Master's thesis, Ruhr Universität, 2006). It can also be assumed that diurnal variations in convective processes would be considerably damped at depths below 3.5 m due to a lack of continuous channels and high ice contents (~85%).

[55] In nature, the degradation at Murtèl rock glacier as seen in the model toward the end of the 21st century will rather lead to a lowering of the surface due to the downwasting of the ice core. So far, this process cannot be simulated with the model used, though. The lateral runoff from the model layers is underestimated by the model below the drainage level. This leads to unrealistically high unfrozen water contents of up to 85% at the Murtèl site after the onset of degradation as meltwater from the ice core is accumulated in the respective layers (see Figure S4).

[56] The simulation of the snow cover trends regarding the duration and the timing of the onset of a continuous snow cover in fall and the date of complete meltoff in spring/summer is consistent with a study by *Bavay et al*. [2008]; similar trends have been found for snow cover duration in Alpine headwater catchments in Switzerland at comparable altitudes. They predicted highly significant changes equal to a shifting of the elevation zone by 900 m with an earlier melt out of the snow cover in spring and mainly liquid precipitation in the fall. Also *Beniston* [2012] found significant snow volume losses of up to 45% at the same altitude range for the Alps by 2100.

6.3. Sensitivity Analysis

[57] The statistical sensitivity study consisting of a multiple regression analysis of up to eight regressors and the dependent variable ALT is a rough approximation to the complex problem of sensitivity. Due to the 1-D approach of the soil model, important 2-D or even 3-D processes such as advective air and water flows cannot be taken into account explicitly. Furthermore, the factors used may counteract each other in the form that warming effects can compensate cooling effects and vice versa.

[58] The number of regressors computed by the stepwise selection differs between the models. Thus, the significance of the influencing factors on ALT varies between the RCMs and the study sites. As the R^2 values are high in general, the statistical models describe the interannual variability of the ALT with good quality for most of the RCMs used. The analysis of the relative importance of the significant factors remaining in the regression models as shown in Figure 7 helps to identify the main influencing factors as well as differences between the two sites. The statistically most significant influencing factors, ice content prior to thawing and summer surface temperature, are of different importance for the permafrost simulations at the respective sites. For both sites, most simulations suggest that ALT variability is mainly depending on the ice content in the active layer.

[59] However, due to the coarse blocky surface layer of most rock glaciers, it is very probable that advective processes, which could not be simulated explicitly in the 1-D subsurface model, will be of additional, if not larger importance for the sensitivity of ALT at Murtèl. Therefore, the obtained sensitivity results have to be interpreted with outmost care.

[60] The ALT of a certain year is shown to influence the ALT of the subsequent years as can be seen in Figure 8. The period for which the influence of a certain thaw depth persists varies between the two study sites. At Schilthorn, the influence of 1 year is only slightly significant for the following years, whereas at Murtèl in most simulations, the influence persists for up to 15 years. However, in case of Schilthorn, the data for this analysis are sparse due to the fact that only years that show a complete refreezing of the active layer are taken into account. Thus, the reliability of the resulting correlations at this site is considered to be weak.

7. Conclusions

[61] In our study, we combined RCM output time series from six different ENSEMBLE scenarios with a sophisticated 1-D subsurface model to analyze the sensitivity of two different mountain permafrost sites to climate change scenarios.

[62] The study showed the general applicability of the combined RCM-permafrost model approach even though the sometimes large uncertainties within the whole model chain have to be considered prior to site-specific interpretation. Furthermore, the 1-D approach of the soil model only allows for the identification of major sensitivity differences between the two sites and does not reflect the real situation in nature. Main findings from the study include the following:

[63] 1. The model shows that the snow cover duration is shortened by 50 to 80 days and the onset of the snow cover in autumn is delayed and the melt out in spring is earlier during the 21st century.

[64] 2. Model results of the hydrothermal regime in the subsurface at both study sites show two phases of permafrost warming and degradation throughout the late 20th and the whole 21st centuries. The first phase is characterized by increasing active layer depths and a warming of the underlying permafrost body. During the second phase, the permafrost becomes inactive, with a continued warming of the permafrost body and positive temperatures persisting in the thawed layer over the years. Due to high uncertainties in the parameterization of the soil and the underestimation of lateral runoff, no explicit conclusions may be drawn concerning the degradation rates.

[65] 3. The simulated permafrost at Schilthorn reacts more sensitive to the projected climate variations than the one at Murtèl, which is most probably due to the differences in the initial ice content at the two sites. At Murtèl, the massive ice core absorbs large amounts of energy. This result is consistent with observations during 2000–2010, where the active layer at Schilthorn shows a much higher sensitivity to comparatively warm years (equal to deepening) than at Murtèl during the same anomalous years [*Hilbich et al*., 2008; *Hoelzle and Gruber*, 2008; *Hilbich et al*., 2009; *PERMOS*, 2010]. It also has to be mentioned that the degradation at Murtèl, as seen in the model, in nature will lead to a lowering of the surface due to downwasting of the ice core and a constant ALT. This process cannot be simulated in the model.

[66] 4. The relative importance of influencing factors on ALT in the permafrost model could be identified qualitatively by a regression analysis. The significance of these factors varies between the six RCMs and the two sites. However, most important factors in the respective simulations are the ice content at the onset of the melting period and the summer surface temperatures followed by days with snow cover and date of melt out of the snow cover. Especially at the Murtèl site, not all processes could be included due to model limitations, so processes important in nature have been neglected.

[67] Perturbations in ALT have shown to be persistent for longer periods of up to 15 years at the Murtèl site. At Schilthorn, ALT variations show no significant influence on ALT of the subsequent years, which is again largely consistent with observations from subsurface temperature measurements within the borehole. On the contrary, interannual ice content changes have been shown to persist over slightly longer periods than temperature anomalies [*Hilbich et al*., 2008].

[68] The influence of climate change, as projected by the six chosen RCMs of the ENSEMBLES project, has been shown to be significant on the simulated permafrost hydrothermal regimes at both sites of this study. Larger impacts were seen at the Schilthorn site, which has low ice contents in the permafrost body and is thus more sensitive. Ice-rich sites as the rock glacier Murtèl is less sensitive to climate warming due to the high amount of energy needed to melt the ice and also because of the special conditions (advective and convective heat fluxes by air and water) within the active layer, representing processes, which were not included in the model used in this study.

[69] In a further step, results from geophysical measurements [*Hilbich et al*., 2011] could be used as 2-D input and validation data for advanced 3-D modeling studies with existing models (e.g., Alpine3D) [*Lehning et al*., 2006]

[70] **Acknowledgments.** We would like to thank the Swiss PERMOS network for data support at the Schilthorn and Murtèl field sites and three anonymous reviewers for their helpful comments which greatly improved the manuscript. We acknowledge the ENSEMBLES project, funded by the European Commission's 6th Framework Programme through contract GOCE-CT-2003-505539. This study was conducted within the bundle project SPCC (Sensitivity of mountain permafrost to climate change) and funded by the German National Science Foundation DFG (grant DFG HA3475/3-1).

References

Anderson, D. M., A. R. Tice, and H. L. McKim (1973), The unfrozen water and the apparent specific heat capacity of frozen soils. In Permafrost: North American Contributions to the Second International Conference, Yakutsk, Siberia, USSR. National Academy of Sciences, Washington, DC, 20418, 289–295.

Arenson, L., M. Hoelzle, and S. Springman (2002), Borehole deformation measurements and internal structure of some rock glaciers in Switzerland. *Permafrost Periglac. Process.*, *13*, 117–135.

Arenson, L. U., and S. M. Springman (2005), Triaxial constant stress and constant strain rate tests on ice-rich permafrost samples, *Canadian Geotechnical Journal*, *42*, 412–430.

Arenson, L. U., M. Phillips, and S. M. Springman (2009), Geotechnical considerations and technical solutions for infrastructure in mountain permafrost, in: M. I. Krugger and H. P. Stern (Eds.), *New Permafrost and Glacier Research*, Nova Science Publishers Inc., New York, 3–50.

Arenson, L., C. Hauck, C. Hilbich, L. Seward, Y. Yamamoto, S. Springman (2010), Sub-surface heterogeneities in the Murtèl-Corvatsch rock glacier, Switzerland, *Geo2010*, *6th Canadian Permafrost Conference*, Calgary, Canada, 1494–1500.

Bavay, M., M. Lehning, T. Jonas, and H. Löwe (2008), Simulations of future snow cover and discharge in Alpine headwater catchments. *Hydrol Processes*, *23*, 95–108.

Beniston, M. (2012), Is snow in the Alps receding or disappearing?, *WIREs Clim. Change*, *3*, 349–358, doi:10.1002/wcc.179.

Boeckli, L., A. Brenning, S. Gruber, and J. Noetzli (2012), A statistical approach to modelling permafrost distribution in the European Alps or

similar mountain ranges, *The Cryosphere*, *6*(1), 125–140, doi:10.5194/tc-6-125-2012.

Christensen, J. H., et al. (2007), Regional climate projections, in *Climate Change 2007: The Physical Science Basis. Contribution of Working Group I to the Fourth Assessment Report of the Intergovernmental Panel on Climate Change*, edited by S. Solomon et al., 847–940, Cambridge Univ. Press, Cambridge, UK and New York, USA.

Dall'Amico, M., S. Endrizzi, S. Gruber, R. Rigon (2011), A robust and energy-conserving model of freezing variably-saturated soil, *The Cryosphere*, *5*, 469–484, doi:10.5194/tc-5-469-2011.

Delaloye, R., and C. Lambiel (2005), Evidence of winter ascending air circulation throughout talus 5 slopes and rock glaciers situated in the lower belt of alpine discontinuous permafrost (Swiss Alps), *Norsk Geogr. Tidsskr.*, *59*, 194–203, 2631, 2644.

Déqué, M., D. P. Rowell, D. Lüthi, F. Giorgi, J. H. Christensen, B. Rockel, D. Jacob, E. Kjellström, M. Castro, and B. Hurk (2007), An intercomparison of regional climate simulations for Europe: Assessing uncertainties in model projections, *Clim. Change*, *81*, 53–70.

Engelhardt, M., C. Hauck and N. Salzmann (2010), Influence of atmospheric forcing parameters on modelled mountain permafrost evolution, *Meteorol. Z.*, *19*, 491–500, doi:10.1127/0941-2948/2010/0476.

Ernst, L.F. (1956), Calculation of the steady flow of groundwater in vertical cross sections, *Netherlands Journal of Agricultural Science*, *4*, 126–131.

Etzelmüller, B., T. V. Schuler, K. Isaksen, H. H. Christiansen, H. Farbrot, R. Benestad (2011), Modeling the temperature evolution of Svalbard permafrost during the 20th and 21st century. *The Cryosphere*, *5*(1), *2011*, 67–79.

Fischer, A. M., A. P. Weigel, C. M. Buser, R. Knutti, H. R. Künsch, M. A. Liniger, C. Schär, and C. Appenzeller (2011), Climate change projections for Switzerland based on a Bayesian multi model approach, *Int. J. Climatol.*, doi:10.1002/joc.3396.

Grömping, U. (2006), Relative importance for linear regression in R: The package relaimpo, *J. Stat. Softw.*, *17*(1), 1–27.

Gruber, S. (2012), Derivation and analysis of a high-resolution estimate of global permafrost zonation, *The Cryosphere*, *6*(1), 221–233, doi:10.5194/tc-6-221-2012.

Haeberli, W., J. Huder, H.-R. Keusen, J. Pica, and H. Röthlisberger (1988), Core drilling through rock–glacier permafrost, In *Proceedings of the Fifth International Conference on Permafrost*, Tapir, Trondheim, 937–942.

Hanson, S., and M. Hoelzle (2003), The thermal regime of the coarse blocky active layer at the Murtèl rock glacier in the Swiss Alps, In *Proceedings of the 8th International Conference on Permafrost, 21–25 July 2003, Zurich*, Edited by: Phillips, M., S. M. Springman, and L. U. Arenson, 51–52, Lisse: A. A. Balkema.

Hanson, S., and M. Hoelzle (2004), The thermal regime of the active layer at the Murtèl rock glacier based on data from 2002, *Permafrost Periglac. Process.*, *15*(3), 273–282.

Harlan, R. L. (1973), Analysis of coupled heat-fluid transport in partially frozen soil, *Water Resour. Res.*, *9*, 1314–1323.

Harris, C., M. C. R. Davies, and B. Etzelmüller (2001a), The assessment of potential geotechnical hazards associated with mountain permafrost in a warming global climate. *Permafrost Periglac Process.*, *12*, 145–156.

Harris, C., W. Haeberli, D. Vonder Mühll, and L. King (2001b), Permafrost monitoring in the high mountains of Europe: The PACE Project in its global context, *Permafrost Periglac. Process.*, *12*(1), 3–12, doi:10.1002/ppp.377.

Hauck, C. (2001), Geophysical methods for detecting permafrost in high mountains, *Mitt. Versuchsanst. Wasserbau*, *Hydrologie und Glaziologie*. ETH Zürich, *171*.

Hawkins, E., and R. Sutton (2009), The potential to narrow uncertainty in regional climate predictions, *Bull. Am. Meteorol. Soc.*, *90*, 1095–1107, doi:10.1175/2009BAMS2607.1.

Hewitt, C. D., and D. J. Griggs (2004), Ensembles-based predictions of climate changes and their impacts, *Eos*, *85*, p. 566.

Hilbich, C., C. Hauck, M. Hoelzle, M. Scherler, L. Schudel, I. Völksch, D. Vonder Mühll, and R. Mäusbacher (2008), Monitoring mountain permafrost evolution using electrical resistivity tomography: A 7-year study of seasonal, annual, and long-term variations at Schilthorn, Swiss Alps, *J. Geophys. Res.*, *113*, F01S90, doi:10.1029/2007JF000799.

Hilbich, C., L. Marescot, C. Hauck, M. Loke, and R. Mäusbacher (2009), Applicability of electrical resistivity tomography monitoring to coarse blocky and ice-rich permafrost landforms. *Permafrost Periglac Process.*, *20*, 269–284, doi:10.1002/ppp.652.

Hilbich, C., C. Fuss, and C. Hauck (2011), Automated time-lapse ERT for improved process analysis and monitoring of frozen ground. *Permafrost and Periglacial Processes*, doi:10.1002/ppp.732.

Hoelzle, M., and W. Haeberli (1995), Simulating the effects of mean annual air temperature changes on permafrost distribution and glacier size: An example from the Upper Engadine, Swiss Alps, *Ann. Glaciol.*, *21*, 399–405.

Hoelzle, M., M. Wegmann, and B. Krummenacher (1999), Miniature temperature dataloggers for mapping and monitoring of permafrost in high mountain areas: First experience from the Swiss Alps, *Permafrost Periglac Process.*, *10*, 113–124.

Hoelzle, M., C. Mittaz, B. Etzelmüller, and W. Haeberli (2001), Surface energy fluxes and distribution models of permafrost in high mountain areas: An overview of current developments, *Permafrost Periglac. Process.*, *12*(1), 53–68.

Hoelzle, M., D. Vonder Mühll, and W. Haeberli (2002), Thirty years of permafrost research in the Corvatsch-Furtshellas area, Eastern Swiss Alps: A review. *Norsk Geogr. Tidsskr.*, *56*, 137–145.

Hoelzle, M., S. Gruber (2008), Borehole and ground surface temperatures and their relationship to meteorological conditions in the Swiss Alps. In *Proceedings Ninth International Conference on Permafrost, June*, 723–728.

Hollesen, J., B. Elberling, and P.-E. Jansson (2011), Future active layer dynamics and carbon dioxide production from thawing permafrost layers in Northeast Greenland, *Glob. Change Biol.*, *17*, 911–926, doi:10.1111/j.1365-2486.2010.02256.X.

Huggel, C. (2008), Recent extreme slope failures in glacial environments: Effects of thermal perturbation, *Quaternary Sci. Rev.*, *28*(11–12), 1119–1130, doi:10.1016/j.quascirev.2008.06.007.

Huggel, C., N. Salzmann, S. Allen, J. Caplan-Auerbach, L. Fischer, W. Haeberli, C. Larsen, D. Schneider, and R. Wessels (2010), Recent and future warm extreme events and high-mountain slope stability, *Philos. T. Roy. Soc. A*, *368*, 2435–2459.

Imhof, M., G. Pierrehumbert, W. Haeberli, and H. Kienholz (2000), Permafrost investigation in the Schilthorn massif, Bernese Alps, Switzerland, *Permafrost Periglac. Process.*, *11*(3), 189–206, doi:10.1002/1099-1530(200007/09)11:3 < 189::AID.-PPP348 > 3.0.CO;2-N.

Isaksen, K., R. S. Oedegard, B. Etzelmueller, C. Hilbich, C. Hauck, E. Farbrot, H. O. Hygen, and T. F. Hipp (2011), Degrading mountain permafrost in southern Norway: Spatial and temporal variability of mean ground temperatures, 1999–2009, *Permafrost Periglac. Process.*, doi:10.1002/ppp.728.

Jansson, P.-E., and L. Karlberg (2004), Coupled heat and mass transfer model for soil-plant-atmosphere systems. Royal Institute of Technology, Dept of Civil and Environmental Engineering, Stockholm.

Jansson, P.-E. (2012), CoupModel: Model use, calibration and validation, *Transactions of the ASABE*, *55*(4), 1335–1344.

Kääb, A., and W. Haeberli (2001), Evolution of a high-mountain thermokarst lake in the Swiss Alps, *Arct. Antarct. Alp. Res.*, *33*, 4, 385–390.

Keller, F. (1992), Automated mapping of mountain permafrost using the program PERMAKART within the geographical information system ARC/INFO. *Permafrost Periglac Process.*, *3*, 133–138, doi:10.1002/ppp.3430030210.

Kudryavtsev, V. A., L. S. Garagulya, K. A. Kondrat'yeva, V. G. Melamed (1974), *Fundamentals of Frost Forecasting in Geological Engineering Investigations*, Cold Regions Research and Engineering Laboratory: Hanover, NH.

Lehning, M., I. Völksch, D. Gustafsson, T. A. Nguyen, M. Stähli, and M. Zappa (2006), ALPINE3D: A detailed model of mountain surface processes and its application to snow hydrology. *Hydrol Processes*, *20*, 2111–2128.

Li, Q., S. Sun, and Y. Xue (2010), Analyses and development of a hierarchy of frozen soil models for cold region study, *J. Geophys. Res.*, *115*, D03107, doi:10.1029/2009JD012530.

Lindeman, R. H., P. F. Merenda, and R. Z. Gold (1980), *Introduction to Bivariate and Multivariate Analysis*, Glenview IL: Scott, Foresman.

Luetschg, M, and W. Haeberli (2005), Permafrost evolution in the Swiss Alps in a changing climate and the role of the snow cover, *Norsk Geografisk Tidsskrift–Norwegian Journal of Geography*, *59*, 78–83.

Luetschg, M., M. Lehning, and W. Haeberli (2008), A sensitivity study of factors influencing warm/thin permafrost in the Swiss Alps. *J. Glaciol.*, *54*, 696–704, doi:10.3189/002214308786570881.

Lunardini, V. J. (1978), Theory of N-factors and correlation of data, in Proceedings of the Third International Conference on Permafrost, Vol. *1*, *National Council of Canada: Ottawa*, 40–46.

Lunardini, V. J. (1981), *Heat Transfer in Cold Climates*, Van Nostrand Reinhold, New York.

Mittaz, C., M. Hoelzle, and W. Haeberli (2000), First results and interpretation of energy-flux measurements over Alpine permafrost, *Ann. Glaciol.*, *31*, 275–280.

Mittaz, C., M. Imhof, M. Hoelzle, and W. Haeberli (2002), Snowmelt evolution mapping using an energy balance approach over an alpine terrain, *Arct. Antarct. Alp. Res.*, *34*(3), 274–281.

Murphy, J. M., D. M. H. Sexton, D. N. Barnett, G. S. Jones, M. J. Webb, M. Collins, and D. A. Stainforth, (2004), Quantification of modelling uncertainties in a large ensemble of climate change simulations, *Nature*, *430*, 768–772.

Nakicenovic, N., et al. (2000), *Special Report on Emissions Scenarios: A Special Report of Working Group III for the Integovernmental Panel on Climate Change*, 599 pp., Cambridge Univ. Press, New York.

Nelson, F. E., and S. I Outcalt. (1987), A computational method for prediction and regionalization of permafrost/A frost index number for spatial prediction of ground frost zones, *Arct. Alp. Res.*, *19*(3), 279–288

PERMOS (2009), *Permafrost in Switzerland 2004/2005 and 2005/2006, Glaciological Report (Permafrost) No. 6/7*, Noetzli J, Naegeli B, Vonder Muehll D (eds), Cryospheric Commission of the Swiss Academy of Sciences, Bern: 100.

PERMOS (2010), *Permafrost in Switzerland 2006/2007 and 2007/2008*, Noetzli, J. and D. Vonder Muehll, (eds.), Glaciological Report (Permafrost) No. 8/9 of the Cryospheric Commission of the Swiss Academy of Sciences, 68 pp.

Phillips, M., E. Zenklusen Mutter, M. Kern-Luetschg, and M. Lehning (2009), Rapid degradation of ground ice in a ventilated talus slope: Flüela Pass, Swiss Alps, *Permafrost Periglac. Process.*, *20*(1), 1–14.

R Development Core Team (2008), R: A language and environment for statistical computing. R Foundation for Statistical Computing, Vienna, Austria, ISBN 3-900051-07-0 [Available at http://www.R-project.org].

Rigon, R., Bertoldi, G., and T. M. Over (2006), GEOtop: A distributed hydrological model with coupled water and energy budgets, *J. Hydrometeorol.*, *7*, 371–388.

Riseborough, D., N. Shiklomanov, B. Etzelmüller, S. Gruber, and S. Marchenko (2008), Recent advances in permafrost modelling, *Permafrost Periglac. Process.*, *19*(2), 137–156, doi:10.1002/ppp.

Romanovsky, V. E., A. L. Kholodov, S. S. Marchenko, N. G. Oberman, D. S. Drozdov, G. V. Malkova, N. G. Moskalenko, A. A. Vasiliev, D. O. Sergeev, and M. N. Zheleznyak (2008), Thermal state and fate of permafrost in Russia: First results of IPY, In *Proceedings of the Ninth International Conference on Permafrost*, *Vol. 2*, Kane D. L., Hinkel K. M. (eds), Institute of Northern Engineering, University of Alaska Fairbanks; 1511–1518.

Salzmann, N., C. Frei, P. L. Vidale, and M. Hoelzle (2007), The application of regional climate model output for the simulation of high-mountain permafrost scenarios. *Global Planet Change*, *56*(1–2), 188–202.

Scherler, M., C. Hauck, M. Hoelzle, M. Stähli, and I. Völksch (2010), Meltwater infiltration into the frozen active layer at an alpine permafrost site. *Permafrost Periglac. Process.*, *21*(4), 325–334, doi:10.1002/ppp.694.

Schneider, S., M. Hoelzle, and C. Hauck (2011), Influence of surface heterogeneity on observed borehole temperatures at a mountain permafrost site in the Upper Engadine Swiss Alps, *The Cryosphere Discuss.*, *5*, 2629–2663, doi:10.5194/tcd-5-2629-2011.

Schwarb, M., C. Daly, C. Frei, and C. Schär (2001), Mean annual and seasonal precipitation in the European Alps 1971–1990, in Hydrological Atlas of Switzerland, Plates 2.6. and 2.7, Landeshydrol. und Geol., Bern.

Smith, L. C., Y. Sheng, G. M. MacDonald, and L. D. Hinzman (2005), Disappearing arctic lakes, *Science*, *308*, 1429.

Smith, M. W., and D. W. Riseborough (1996), Ground temperature monitoring and detection of climate change, *Permafrost Periglac. Process.*, *7*(4), 301–310, doi:10.1002/(SICI)1099-1530(199610)7:4 < 301::AID-PPP231 > 3.0.CO;2-R.

Solomon, S., D. Qin, M. Manning, Z. Chen, M. Marquis, K. B. Averyt, M. Tignor, and H. L. Miller, editors (2007),*Contribution of Working Group I to the Fourth Assessment Report of the Intergovernmental Panel on Climate Change*. Cambridge University Press, Cambridge, United Kingdom and New York, NY, USA, 2007.

Stocker-Mittaz, C. (2002), Permafrost distribution modeling based on energy balance data, Ph.D. thesis, Univ. of Zurich, Zurich, Switzerland.

Van der Linden, P., and J. F. B. Mitchell (2009), ENSEMBLES: Climate change and its impacts: Summary of research and results from the ENSEMBLES project, Met Office Hadley Centre, FitzRoy Road, Exeter EX1 3 PB, UK. 2009.

Venables, W. N., and B. D. Ripley (2002), *Modern Applied Statistics with S*, Fourth Edition, Springer, New York, ISBN 0-387-95457-0.

Voelksch, I., and M. Lehning (2005), Model assessment of permafrost development for a large alpine catchment, American Geophysical Union, Fall Meeting 2005, abstract #C23B-07.

Vonder Mühll, D., and P. Holub (1992), Borehole logging in Alpine permafrost, Upper Engadine, Swiss Alps. *Permafrost Periglac Process.*, *3*, 125–132.

Wu, Q., and T. Zhang (2008), Recent permafrost warming on the Qinghai-Tibetan Plateau, *J. Geophys. Res.*, *113*, D13108, doi:10.1029/2007JD009539.

Yoshikawa, K., and L. D. Hinzman (2003), Shrinking thermokarst ponds and groundwater dynamics in discontinuous permafrost near Council, Alaska. *Permafrost Periglac Process.*, *14*, 151–160.

Zenklusen, E., and M. Phillips (2012), Active layer characteristics at ten borehole sites in alpine permafrost terrain, *Permafrost and Periglacial Processes*, Switzerland, *23*(2), 138–151, ISSN 1099–1530. doi:10.1002/ppp.1738. [Available at http://dx.doi.org/10.1002/ppp.1738].

Zhang, T., R. Barry, and W. Haeberli (2001), Numerical simulations of the influence of the seasonal snow cover on the occurrence of permafrost at high latitudes, *Norsk Geogr. Tidsskr.*, *55*(4), 261–266.